sciendo

Int. J. Appl. Math. Comput. Sci., 2022, Vol. 32, No. 2, 171–183
DOI: 10.34768/amcs-2022-0013

amcs

FAULT–TOLERANT TRACKING CONTROL FOR A NON–LINEAR TWIN–ROTOR SYSTEM UNDER ELLIPSOIDAL BOUNDING

NORBERT KUKUROWSKI [a,*], MARCIN MRUGALSKI [a], MARCIN PAZERA [a], MARCIN WITCZAK [a]

[a]Institute of Control and Computation Engineering
University of Zielona Góra
Szafrana 2, 65-516 Zielona Góra, Poland
e-mail: {n.kukurowski,m.mrugalski}@issi.uz.zgora.pl,
{m.pazera,m.witczak}@issi.uz.zgora.pl

A novel fault-tolerant tracking control scheme based on an adaptive robust observer for non-linear systems is proposed. Additionally, it is presumed that the non-linear system may be faulty, i.e., affected by actuator and sensor faults along with the disturbances, simultaneously. Accordingly, the stability of the robust observer as well as the fault-tolerant tracking controller is achieved by using the $\mathcal{H}_\infty$ approach. Furthermore, unknown actuator and sensor faults and states are bounded by the uncertainty intervals for estimation quality assessment as well as reliable fault diagnosis. This means that narrow intervals accompany better estimation quality. Thus, to cope with the above difficulty, it is assumed that the disturbances are over-bounded by an ellipsoid. Consequently, the performance and correctness of the proposed fault-tolerant tracking control scheme are verified by using a non-linear twin-rotor aerodynamical laboratory system.

Keywords: fault-tolerant control, simultaneous faults, external disturbances, non-linear system, robust fault estimation, fault detection and diagnosis.

1. Introduction

Currently, a rapid development of unmanned land, underwater and aerial vehicles can be observed (Liu *et al*., 2021; Altan and Hacıoğlu, 2020; Wang, 2020; Tang *et al*., 2021; Witczak *et al*., 2020; Sun and Liu, 2021). These vehicles are equipped with numerous sensors and actuators. Such components are used to recognize the surrounding environment, perform missions, communicate and control vehicles remotely or autonomously. Modern autonomous vehicles must be able to react quickly in a changing environment. Due to the high cost of modern autonomous vehicles, long-term durability and reliability are expected from them. Moreover, in the event of a fault of one or more components of the autonomous vehicle, the ability to continue the mission or at least safely return to the place where it started is expected.

In the case of unmanned aerial vehicles (UAVs), the problem of ensuring reliability and control (Abbaspour *et al*., 2018; Hamadi *et al*., 2020; Altan and Hacıoğlu, 2020; Prochazka and Stomberg, 2020; Taimoor *et al*., 2021) is particularly important because they are characterized by high dynamics and functioning in varying conditions with a large amount of disturbances. In order to ensure the reliable operation of a UAV, various methods of fault detection and estimation of the remaining useful life of the vehicle components can be used (Zhang *et al*., 2021; Sadhu *et al*., 2020; Camci *et al*., 2019; Rodrigues *et al*., 2018; Petritoli *et al*., 2018). This knowledge enables early detection of the deteriorating quality of individual vehicle components and their earlier replacement before their faults could lead to a failure of the UAV.

Unfortunately, even the most advanced fault diagnosis and the remaining useful life estimates are not able to prevent random events leading to faults of the UAV. The occurrence of weather disturbances may lead to a deterioration of the quality parameters of the system, some sensors or actuators made during the mission. It should be emphasized that modern vehicles

*Corresponding author

have redundant equipment, which, with the availability of appropriate fault-tolerant control (FTC) methods allows for the continuation of the mission (Camci *et al*., 2019).

There are many FTC methods in the literature, among which there are passive (Saied *et al*., 2020; Vural *et al*., 2018; Patel and Shah, 2019) and active methods (Abbaspour *et al*., 2018; Nguyen *et al*., 2017; Chung and Son, 2020; Kukurowski *et al*., 2021). For the first of them, the properly designed controllers allow us to achieve certain parameters in both normal and faulty cases. On the other hand, in the case of faults the active FTC approach modifies the controller parameters or, in some cases, its structure. This type of FTC requires an appropriate designed fault detection and identification (FDI) subsystem (Hu *et al*., 2021; Mrugalski, 2014; Chen *et al*., 2019). An overview of FTC methods can be found the works of Veremey (2021), Habibi *et al*. (2019), Li *et al*. (2019), Hamdi *et al*. (2021) and Witczak (2014). Moreover, interesting theoretical studies and practical applications of active FTC methods in the case of faulty sensors (Manohar and Das, 2020; Wang, 2020; Azzoug *et al*., 2021; Taimoor *et al*., 2021) and actuators (Hamadi *et al*., 2020; Prochazka and Stomberg, 2020; Yu *et al*., 2021; Liu *et al*., 2021) can also be found.

In this article a new FTC method based on a two-step action is proposed. In the first stage, an observer for nonlinear systems is developed, enabling the estimation of the state, sensor and actuator faults, robust against to disturbances and noise. In the second stage, based on the obtained observer, a fault-tolerant tracking controller (FTTC) is proposed. It is designed to allow minimization of the error between the reference state and the state of the faulty system. It is worth noting that the stability of both solutions is achieved through the use of the H_∞ approach (Witczak *et al*., 2014). In the design of the gain matrices of the observer and the controller, the LMI method is used. In order to ensure that the proposed solution is reliable during fault diagnosis, a method of determining the uncertainty intervals based on the limitation of external disturbances by means of ellipsoids is proposed. It is worth mentioning that the proposed approach also allows for the assessment of the estimation quality of states, sensors and actuators. Finally, the proposed approach was applied to the fault tolerant control of the sixth-order highly nonlinear model of a twin rotor aerodynamical laboratory system in order to show its efficiency and robustness against external disturbances.

The paper is organized as follows. In Section 2 a new scheme of the fault-tolerant tracking controller is proposed along with its design. In Section 3 a methodology of determination of uncertainty intervals is outlined. In Section 4 the performance of the proposed FTC strategy is confirmed on a laboratory twin-rotor aerodynamical system. Finally, in Section 5 conclusions are included.

2. Fault-tolerant tracking controller design

Consider the following nonlinear system with faults and uncertainties:

$$\begin{aligned} \boldsymbol{x}_{f,k+1} &= \boldsymbol{A}\boldsymbol{x}_{f,k} + \boldsymbol{B}\boldsymbol{u}_{f,k} + \boldsymbol{B}\boldsymbol{f}_{a,k} + \boldsymbol{q}\left(\boldsymbol{x}_{f,k}\right) \\ &\quad + \boldsymbol{W}_1\boldsymbol{w}_{1,k}, \end{aligned} \tag{1}$$

$$\boldsymbol{y}_{f,k} = \boldsymbol{C}\boldsymbol{x}_{f,k} + \boldsymbol{C}_f\boldsymbol{f}_{s,k} + \boldsymbol{W}_2\boldsymbol{w}_{2,k}, \tag{2}$$

where $\boldsymbol{u}_{f,k} \in \mathbb{R}^r$, $\boldsymbol{x}_{f,k} \in \mathbb{X} \subset \mathbb{R}^n$, $\boldsymbol{y}_{f,k} \in \mathbb{R}^m$ denote the input, state and output, respectively. Additionally, it is assumed that the system may be influenced by actuator and sensor faults given with $\boldsymbol{f}_{a,k} \in \mathbb{F}_a \subset \mathbb{R}^{n_a}$ and $\boldsymbol{f}_{s,k} \in \mathbb{F}_s \subset \mathbb{R}^{n_s}$, respectively. Accordingly, the sensor fault distribution matrix is defined by $\boldsymbol{C}_f$ with $\text{rank}(\boldsymbol{C}_f) = n_s$. Furthermore, $\boldsymbol{q}\left(\boldsymbol{x}_{f,k}\right) : \mathbb{X} \to \mathbb{X}$ is a nonlinear function of the state. Finally, $\boldsymbol{w}_{1,k}$ and $\boldsymbol{w}_{2,k}$ are exogenous disturbance vectors; they indicate the process and measurement uncertainties, along with their distribution matrices $\boldsymbol{W}_1$ and $\boldsymbol{W}_2$, respectively. For further deliberations, recall the following result, which will be used to cope with nonlinearities.

Lemma 1. (Zemouche and Boutayeb, 2013) *For $\boldsymbol{q}(\cdot)$, the following statements are equivalent*

1. *$\boldsymbol{q}(\cdot)$ is Lipschitz with Lipschitz constant $\gamma_h > 0$, i.e.,*

$$\| \boldsymbol{q}(\boldsymbol{X}) - \boldsymbol{q}(\boldsymbol{Y}) \| \leq \gamma_h \| \boldsymbol{X} - \boldsymbol{Y} \|, \quad \forall \boldsymbol{X}, \boldsymbol{Y} \in \mathbb{X}.$$

2. *For all $i, j = 1, \ldots, n$, there exist functions $h_{i,j} : \mathbb{X} \times \mathbb{X} \to \mathbb{R}$ and constants $\underline{\gamma}_{h_{i,j}}$ and $\bar{\gamma}_{h_{i,j}}$ such that for each $\boldsymbol{X}, \boldsymbol{Y} \in \mathbb{X}$*

$$\boldsymbol{q}(\boldsymbol{X}) - \boldsymbol{q}(\boldsymbol{Y}) = \sum_{i=1}^{n}\sum_{j=1}^{n} h_{i,j}\boldsymbol{H}_{i,j}\left(\boldsymbol{X} - \boldsymbol{Y}\right), \tag{3}$$

and

$$\underline{\gamma}_{h,i,j} \leq h_{i,j} \leq \bar{\gamma}_{h,i,j}, \tag{4}$$

$$h_{i,j} \triangleq h_{i,j}\left(\boldsymbol{X}^{\boldsymbol{Y}_{j-1}}, \boldsymbol{X}^{\boldsymbol{Y}_j}\right), \qquad \boldsymbol{H}_{i,j} = \boldsymbol{c}_i\boldsymbol{c}_i^T.$$

Specifically,

$$h_{ij}\left(\boldsymbol{X}^{\boldsymbol{Y}_{j-1}}, \boldsymbol{X}^{\boldsymbol{Y}_j}\right) = \begin{cases} \boldsymbol{0} & \text{if } x_{f,j} = y_{f,j}, \\ \frac{\boldsymbol{g}_i\left(\boldsymbol{X}^{\boldsymbol{Y}_{j-1}}\right) - \boldsymbol{g}_i\left(\boldsymbol{X}^{\boldsymbol{Y}_j}\right)}{x_{f,j} - y_{f,j}} & \text{if } x_{f,j} \neq y_{f,j}, \end{cases} \tag{5}$$

where $\boldsymbol{c}_i$ stands for the i-th column of the identity

matrix of size n while $\boldsymbol{X}^{\boldsymbol{Y}_i}$ is defined by

$$\boldsymbol{X}^{\boldsymbol{Y}_i} = \begin{bmatrix} y_{f,1} \\ \vdots \\ y_{f,i} \\ x_{f,i+1} \\ \vdots \\ x_{f,n} \end{bmatrix} \quad \textit{for} \;\; i = 1, \ldots, n, \tag{6}$$

$$\boldsymbol{X}^{\boldsymbol{Y}_0} = \boldsymbol{X}. \tag{7}$$

2.1. Example application of Lemma 1. To make the entire presentation clearer, consider an illustrative example in which the nonlinear vector function is

$$\boldsymbol{q}\,(\boldsymbol{X}) = [\sin(x_1)\cos(x_2), \cos(x_2)]^T, \tag{8}$$

where $\boldsymbol{X} = [x_1, x_2]^T$. Also define a vector $\boldsymbol{Y} = [y_1, y_2]^T$. Thus, according to (6) and (7),

$$\boldsymbol{X}^{\boldsymbol{Y}_0} = [x_1, x_2]^T, \tag{9}$$

$$\boldsymbol{X}^{\boldsymbol{Y}_1} = [y_1, x_2]^T, \tag{10}$$

$$\boldsymbol{X}^{\boldsymbol{Y}_2} = [y_1, y_2]^T. \tag{11}$$

Consequently, as a result of applying (5), it is easy to see that

$$h_{1,1} = \begin{cases} 0 & \text{if } x_2 = y_2, \\ \dfrac{-\sin(y_1)\cos(x_2) + \sin(x_1)\cos(x_2)}{x_1 - y_1} & \text{if } x_1 \neq y_1, \end{cases} \tag{12}$$

$$h_{1,2} = \begin{cases} 0 & \text{if } x_2 = y_2, \\ \dfrac{-\sin(y_1)\cos(y_2) + \sin(y_1)\cos(x_2)}{x_2 - y_2} & \text{if } x_2 \neq y_2, \end{cases} \tag{13}$$

$$h_{2,1} = 0, \tag{14}$$

$$h_{2,2} = \begin{cases} 0 & \text{if } x_2 = y_2, \\ \dfrac{\cos(x_2) - \cos(y_2)}{x_2 - y_2} & \text{if } x_2 \neq y_2. \end{cases} \tag{15}$$

Substituting (12)–(15) into (3), we can easily see that the equality holds. However, to obtain the final linear parameter-varying form, it is crucial to determine the bounds defined by (4). This task can realized through the nonlinear optimization of (12)–(15) subject to the constraint $\boldsymbol{X} \in \mathbb{X}$.

2.2. Main results. As a result of applying Lemma 1, the following relations can be determined:

$$\boldsymbol{q}\,(\boldsymbol{x}_{f,k}) - \boldsymbol{q}\,(\hat{\boldsymbol{x}}_{f,k}) = \boldsymbol{G}(\boldsymbol{h})(\boldsymbol{x}_{f,k} - \hat{\boldsymbol{x}}_{f,k}), \tag{16}$$

$$\boldsymbol{q}\,(\boldsymbol{x}_k) - \boldsymbol{q}\,(\boldsymbol{x}_{f,k}) = \boldsymbol{Q}(\boldsymbol{h})(\boldsymbol{x}_k - \boldsymbol{x}_{f,k}), \tag{17}$$

where $\hat{\boldsymbol{x}}_k$ is the state estimate while

$$\boldsymbol{G}(\boldsymbol{h}) = \sum_{i=1}^{n}\sum_{j=1}^{n} h_{i,j}\boldsymbol{H}_{i,j}, \tag{18}$$

$$\underline{\gamma}_{h,i,j} \leq h_{i,j} \leq \bar{\gamma}_{h,i,j}.$$

The main objective of this paper is to propose an FTTC scheme based on state and fault estimates. Thus, the proposed strategy will allow the FTC controller to reduce the tracking error across a reference state $\boldsymbol{x}_k$ and the state $\boldsymbol{x}_{f,k}$, which may be influenced by actuator and sensor faults. Additionally, it is assumed that in the system a nominal controller is already employed, which will be not changed due to the proposed FTC strategy. Accordingly, the proposed FTC scheme for nonlinear model can be illustrated by a schematic diagram of Fig. 1.

Thus, assume that a nominal controller is already exists in the system and it can be in the form of the simple state feedback controller

$$\boldsymbol{u}_k = -\boldsymbol{K}\boldsymbol{x}_k, \tag{19}$$

where $\boldsymbol{K}$ signifies the gain matrix. Additionally, the purpose is to expand the system with another controller

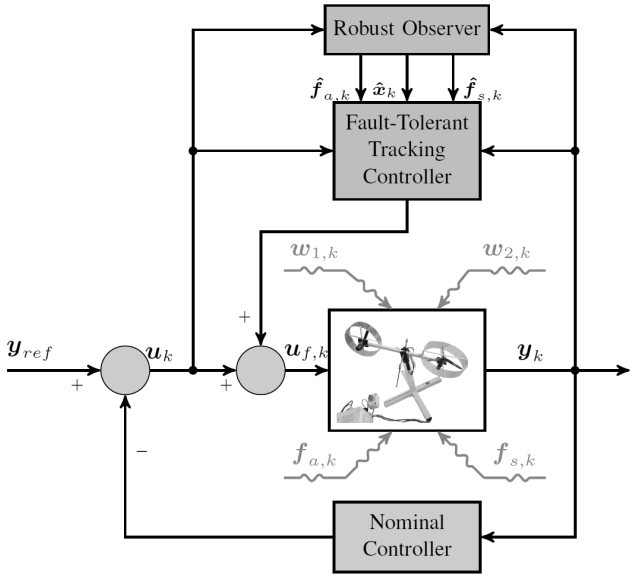

Fig. 1. Scheme of the tracking fault-tolerant control.

which will be capable of reducing the tracking error. Therefore, consider the following reference system:

$$\boldsymbol{x}_{k+1} = \boldsymbol{A}\boldsymbol{x}_k + \boldsymbol{B}\boldsymbol{u}_k + \boldsymbol{q}\left(\boldsymbol{x}_k\right), \tag{20}$$

$$\boldsymbol{y}_k = \boldsymbol{C}\boldsymbol{x}_k, \tag{21}$$

where $\boldsymbol{u}_k \in \mathbb{R}^r$, $\boldsymbol{x}_k \in \mathbb{R}^n$ and $\boldsymbol{y}_k \in \mathbb{R}^m$ denote the control input of the nominal controller (19), reference state and output, respectively. Moreover, $\boldsymbol{q}\left(\boldsymbol{x}_{f,k}\right) : \mathbb{X} \to \mathbb{X}$ defines a nonlinear function.

The fundamental idea is to propose the FTC strategy for the possibly faulty system (1)–(2) as

$$\boldsymbol{u}_{f,k} = -\hat{\boldsymbol{f}}_{a,k} + \boldsymbol{K}_c\left(\boldsymbol{x}_k - \hat{\boldsymbol{x}}_{f,k}\right) + \boldsymbol{u}_k, \tag{22}$$

where $\hat{\boldsymbol{f}}_{a,k}$ indicates the actuator fault estimate and $\boldsymbol{K}_c$ denotes the gain matrix. It should be noted that the observer state $\hat{\boldsymbol{x}}_{f,k}$ may be used when $\boldsymbol{x}_{f,k}$ is not accessible. Thus, we propose the following state, sensor and actuator fault estimates:

$$\begin{aligned}\hat{\boldsymbol{x}}_{f,k+1} = {} & \boldsymbol{A}\hat{\boldsymbol{x}}_k + \boldsymbol{B}\boldsymbol{u}_k + \boldsymbol{B}\hat{\boldsymbol{f}}_{a,k} + \boldsymbol{q}\left(\hat{\boldsymbol{x}}_{f,k}\right) \\ & + \boldsymbol{K}_x\left(\boldsymbol{y}_k - \boldsymbol{C}\hat{\boldsymbol{x}}_k - \boldsymbol{C}_f\hat{\boldsymbol{f}}_{s,k}\right),\end{aligned} \tag{23}$$

$$\hat{\boldsymbol{f}}_{a,k+1} = \hat{\boldsymbol{f}}_{a,k} + \boldsymbol{K}_a\left(\boldsymbol{y}_k - \boldsymbol{C}\hat{\boldsymbol{x}}_k - \boldsymbol{C}_f\hat{\boldsymbol{f}}_{s,k}\right), \tag{24}$$

$$\hat{\boldsymbol{f}}_{s,k+1} = \hat{\boldsymbol{f}}_{s,k} + \boldsymbol{K}_s\left(\boldsymbol{y}_k - \boldsymbol{C}\hat{\boldsymbol{x}}_k - \boldsymbol{C}_f\hat{\boldsymbol{f}}_{s,k}\right). \tag{25}$$

Replacing (22) into (1) yields

$$\begin{aligned}\boldsymbol{x}_{f,k+1} = {} & \boldsymbol{A}\boldsymbol{x}_{f,k} - \boldsymbol{B}\hat{\boldsymbol{f}}_{a,k} \\ & + \boldsymbol{B}\boldsymbol{K}_c\left(\boldsymbol{e}_k - \boldsymbol{e}_{f,k}\right) + \boldsymbol{B}\boldsymbol{u}_k \\ & + \boldsymbol{B}\boldsymbol{f}_{a,k} + \boldsymbol{q}\left(\boldsymbol{x}_{f,k}\right) + \boldsymbol{W}_1\boldsymbol{w}_{1,k},\end{aligned} \tag{26}$$

along with

$$\boldsymbol{e}_k = \boldsymbol{x}_k - \boldsymbol{x}_{f,k}, \qquad \boldsymbol{e}_{f,k} = \boldsymbol{x}_{f,k} - \hat{\boldsymbol{x}}_{f,k}, \tag{27}$$

where $\boldsymbol{e}_k$ is the tracking error and $\boldsymbol{e}_{f,k}$ signifies the estimation error. Hence

$$\begin{aligned}\boldsymbol{x}_{f,k+1} = {} & \boldsymbol{A}\boldsymbol{x}_{f,k} + \boldsymbol{B}\boldsymbol{e}_{a,k} \\ & + \boldsymbol{B}\boldsymbol{K}_c\left(\boldsymbol{e}_k - \boldsymbol{e}_{f,k}\right) + \boldsymbol{B}\boldsymbol{u}_k \\ & + \boldsymbol{q}\left(\boldsymbol{x}_{f,k}\right) + \boldsymbol{W}_1\boldsymbol{w}_{1,k},\end{aligned} \tag{28}$$

where $\boldsymbol{e}_{a,k}$ indicates the actuator fault estimation error.

Let the tracking and state estimation error be defined as

$$\begin{aligned}\boldsymbol{e}_{k+1} = {} & \boldsymbol{x}_{k+1} - \boldsymbol{x}_{f,k+1} \\ = {} & \left(\boldsymbol{A} - \boldsymbol{B}\boldsymbol{K}_c\right)\boldsymbol{e}_k \\ & - \boldsymbol{B}\boldsymbol{e}_{a,k} - \boldsymbol{B}\boldsymbol{K}_c\boldsymbol{e}_{f,k} \\ & + \boldsymbol{q}\left(\boldsymbol{x}_k\right) - \boldsymbol{q}\left(\boldsymbol{x}_{f,k}\right) - \boldsymbol{W}_1\boldsymbol{w}_{1,k},\end{aligned} \tag{29}$$

$$\begin{aligned}\boldsymbol{e}_{f,k+1} = {} & \boldsymbol{x}_{f,k+1} - \hat{\boldsymbol{x}}_{f,k+1} \\ = {} & \left(\boldsymbol{A} - \boldsymbol{K}_x\boldsymbol{C}\right)\boldsymbol{e}_{f,k} \\ & + \boldsymbol{B}\boldsymbol{e}_{a,k} - \boldsymbol{K}_x\boldsymbol{C}_f\boldsymbol{e}_{s,k} \\ & + \boldsymbol{q}\left(\boldsymbol{x}_{f,k}\right) - \boldsymbol{q}\left(\hat{\boldsymbol{x}}_{f,k}\right) \\ & + \boldsymbol{W}_1\boldsymbol{w}_{1,k} - \boldsymbol{K}_x\boldsymbol{W}_2\boldsymbol{w}_{2,k}.\end{aligned} \tag{30}$$

Accordingly, let the actuator and sensor fault estimates be defined as

$$\begin{aligned}\boldsymbol{e}_{a,k+1} = {} & \boldsymbol{f}_{a,k+1} - \hat{\boldsymbol{f}}_{a,k+1} \\ = {} & \boldsymbol{\varepsilon}_{a,k} + \boldsymbol{e}_{a,k} - \boldsymbol{K}_a\boldsymbol{C}\boldsymbol{e}_{f,k} \\ & - \boldsymbol{K}_a\boldsymbol{C}_f\boldsymbol{e}_{s,k} - \boldsymbol{K}_a\boldsymbol{W}_2\boldsymbol{w}_{2,k},\end{aligned} \tag{31}$$

$$\begin{aligned}\boldsymbol{e}_{s,k+1} = {} & \boldsymbol{f}_{s,k+1} - \hat{\boldsymbol{f}}_{s,k+1} \\ = {} & \boldsymbol{\varepsilon}_{s,k} + \left(\boldsymbol{I} - \boldsymbol{K}_s\boldsymbol{C}_f\right)\boldsymbol{e}_{s,k} \\ & - \boldsymbol{K}_s\boldsymbol{C}\boldsymbol{e}_{f,k} - \boldsymbol{K}_s\boldsymbol{W}_2\boldsymbol{w}_{2,k},\end{aligned} \tag{32}$$

where

$$\boldsymbol{\varepsilon}_{a,k} = \boldsymbol{f}_{a,k+1} - \boldsymbol{f}_{a,k}, \quad \boldsymbol{\varepsilon}_{s,k} = \boldsymbol{f}_{s,k+1} - \boldsymbol{f}_{s,k}.$$

Furthermore, we form the following super-vectors by stacking (29)–(32):

$$\bar{\boldsymbol{e}}_k = \begin{bmatrix}\boldsymbol{e}_k \\ \boldsymbol{e}_{f,k} \\ \boldsymbol{e}_{a,k} \\ \boldsymbol{e}_{s,k}\end{bmatrix}, \quad \bar{\boldsymbol{w}}_k = \begin{bmatrix}\boldsymbol{w}_{1,k} \\ \boldsymbol{w}_{2,k} \\ \boldsymbol{\varepsilon}_{a,k} \\ \boldsymbol{\varepsilon}_{s,k}\end{bmatrix}. \tag{33}$$

In consequence the state estimation error can be described in the following compact form:

$$\begin{aligned}\bar{\boldsymbol{e}}_{k+1} = {} & \begin{bmatrix}\boldsymbol{A} - \boldsymbol{B}\boldsymbol{K}_c + \boldsymbol{X}(\boldsymbol{h}) & -\boldsymbol{B}\boldsymbol{K}_c \\ \boldsymbol{0} & \boldsymbol{A} - \boldsymbol{K}_x\boldsymbol{C} + \boldsymbol{G}(\boldsymbol{h}) \\ \boldsymbol{0} & -\boldsymbol{K}_a\boldsymbol{C} \\ \boldsymbol{0} & -\boldsymbol{K}_s\boldsymbol{C}\end{bmatrix} \\ & \begin{bmatrix}-\boldsymbol{B} & \boldsymbol{0} \\ \boldsymbol{B} & -\boldsymbol{K}_x\boldsymbol{C}_f \\ \boldsymbol{I} & -\boldsymbol{K}_a\boldsymbol{C}_f \\ \boldsymbol{0} & \boldsymbol{I} - \boldsymbol{K}_s\boldsymbol{C}_f\end{bmatrix}\bar{\boldsymbol{e}}_k \\ & + \begin{bmatrix}-\boldsymbol{W}_1 & \boldsymbol{0} & \boldsymbol{0} & \boldsymbol{0} \\ \boldsymbol{W}_1 & -\boldsymbol{K}_x\boldsymbol{W}_2 & \boldsymbol{0} & \boldsymbol{0} \\ \boldsymbol{0} & -\boldsymbol{K}_a\boldsymbol{W}_2 & \boldsymbol{I} & \boldsymbol{0} \\ \boldsymbol{0} & -\boldsymbol{K}_s\boldsymbol{W}_2 & \boldsymbol{0} & \boldsymbol{I}\end{bmatrix}\bar{\boldsymbol{w}}_k,\end{aligned} \tag{34}$$

or simply as

$$\bar{\boldsymbol{e}}_{k+1} = \tilde{\boldsymbol{A}}_1(\boldsymbol{h})\bar{\boldsymbol{e}}_k + \tilde{\boldsymbol{W}}_1\bar{\boldsymbol{w}}_k, \tag{35}$$

where

$$\begin{aligned}
\tilde{\boldsymbol{A}}_1(\boldsymbol{h}) &= \begin{bmatrix} \bar{\boldsymbol{A}}_1(\boldsymbol{h}) & \bar{\boldsymbol{B}} \\ \boldsymbol{0} & \bar{\boldsymbol{A}}_2(\boldsymbol{h}) \end{bmatrix}, \\
\tilde{\boldsymbol{W}}_1 &= \begin{bmatrix} -\boldsymbol{W}_1 & \boldsymbol{0} \\ \bar{\boldsymbol{W}}_1 & \bar{\boldsymbol{W}}_2 \end{bmatrix}, \\
\bar{\boldsymbol{W}}_2 &= \bar{\boldsymbol{W}}_3 - \bar{\boldsymbol{K}}\tilde{\boldsymbol{W}}_2, \\
\tilde{\boldsymbol{W}}_2 &= \begin{bmatrix} \boldsymbol{W}_2 & \boldsymbol{0} & \boldsymbol{0} \end{bmatrix}, \\
\bar{\boldsymbol{A}}_1(\boldsymbol{h}) &= \boldsymbol{A} - \boldsymbol{B}\boldsymbol{K}_c + \boldsymbol{X}(\boldsymbol{h}), \\
\bar{\boldsymbol{B}} &= \begin{bmatrix} -\boldsymbol{B}\boldsymbol{K}_c & -\boldsymbol{B} & \boldsymbol{0} \end{bmatrix}, \\
\bar{\boldsymbol{W}}_1 &= \begin{bmatrix} \boldsymbol{W}_1^T & \boldsymbol{0} & \boldsymbol{0} \end{bmatrix}^T, \\
\bar{\boldsymbol{W}}_3 &= \begin{bmatrix} \boldsymbol{0} & \boldsymbol{0} & \boldsymbol{0} \\ \boldsymbol{0} & \boldsymbol{I} & \boldsymbol{0} \\ \boldsymbol{0} & \boldsymbol{0} & \boldsymbol{I} \end{bmatrix}, \\
\bar{\boldsymbol{K}} &= \begin{bmatrix} \boldsymbol{K}_x^T & \boldsymbol{K}_a^T & \boldsymbol{K}_s^T \end{bmatrix}^T.
\end{aligned}$$

It is easily seen that the observer and the fault-tolerant controller may be designed separately due to the fact that the eigenvalues of $\tilde{\boldsymbol{A}}_1(\boldsymbol{h})$ depend on the ones of $\bar{\boldsymbol{A}}_1(\boldsymbol{h})$ and $\bar{\boldsymbol{A}}_2(\boldsymbol{h})$. Accordingly, rewrite

$$\bar{\boldsymbol{A}}_2(\boldsymbol{h}) = \begin{bmatrix} \boldsymbol{A} - \boldsymbol{K}_x\boldsymbol{C} + \boldsymbol{G}(\boldsymbol{h}) & \boldsymbol{B} & -\boldsymbol{K}_x\boldsymbol{C}_f \\ -\boldsymbol{K}_a\boldsymbol{C} & \boldsymbol{I} & -\boldsymbol{K}_a\boldsymbol{C}_f \\ -\boldsymbol{K}_s\boldsymbol{C} & \boldsymbol{0} & \boldsymbol{I} - \boldsymbol{K}_s\boldsymbol{C}_f \end{bmatrix}$$

in the simpler form

$$\bar{\boldsymbol{A}}_2(\boldsymbol{h}) = \bar{\boldsymbol{A}}(\boldsymbol{h}) - \bar{\boldsymbol{K}}\bar{\boldsymbol{C}},$$

where

$$\begin{aligned}
\bar{\boldsymbol{A}}(\boldsymbol{h}) &= \begin{bmatrix} \boldsymbol{A} + \boldsymbol{G}(\boldsymbol{h}) & \boldsymbol{B} & \boldsymbol{0} \\ \boldsymbol{0} & \boldsymbol{I} & \boldsymbol{0} \\ \boldsymbol{0} & \boldsymbol{0} & \boldsymbol{I} \end{bmatrix}, \\
\bar{\boldsymbol{C}} &= \begin{bmatrix} \boldsymbol{C} & \boldsymbol{0} & \boldsymbol{C}_f \end{bmatrix}.
\end{aligned}$$

As a result, the observer can be defined as

$$\tilde{\boldsymbol{e}}_{f,k+1} = \bar{\boldsymbol{A}}_2(\boldsymbol{h})\tilde{\boldsymbol{e}}_{f,k} + \bar{\boldsymbol{W}}_2\bar{\boldsymbol{w}}_k, \tag{36}$$

where

$$\tilde{\boldsymbol{e}}_{f,k} = \begin{bmatrix} \boldsymbol{e}_{f,k}^T, \boldsymbol{e}_{a,k}^T, \boldsymbol{e}_{s,k}^T \end{bmatrix}^T.$$

Based on the above, recall the Lyapunov function

$$V_{f,k} = \tilde{\boldsymbol{e}}_{f,k}^T\boldsymbol{P}_f\tilde{\boldsymbol{e}}_{f,k}, \tag{37}$$

with $\boldsymbol{P}_f \succ 0$. Moreover, assume that $\bar{\boldsymbol{w}}_k \in l_2$ while

$$l_2 = \left\{ \mathbf{w} \in \mathbb{R}^n | \ \|\mathbf{w}\|_{l_2} < +\infty \right\}, \tag{38}$$

with

$$\|\mathbf{w}\|_{l_2} = \left(\sum_{k=0}^{\infty} \|\boldsymbol{w}_k\|^2 \right)^{\frac{1}{2}}. \tag{39}$$

Additionally, it is assumed that $\bar{\boldsymbol{w}}_k$ is overbounded by an ellipsoid such as

$$\mathbb{E}_w = \left\{ \bar{\boldsymbol{w}}_k : \ \bar{\boldsymbol{w}}_k^T \frac{\mu_f^2}{\alpha} \boldsymbol{I} \bar{\boldsymbol{w}}_k \leq 1 \right\}, \tag{40}$$

whilst

$$\frac{\mu_f^2}{\alpha}\boldsymbol{I} \succ 0.$$

Based on the above, the stability condition is defined by

$$\Delta V_{f,k} + \tilde{\boldsymbol{e}}_{f,k}^T\tilde{\boldsymbol{e}}_{f,k} - \mu_f^2\bar{\boldsymbol{w}}_k^T\bar{\boldsymbol{w}}_k < 0, \tag{41}$$

along with

$$\begin{aligned}
\Delta V_{f,k} &= V_{f,k+1} - V_{f,k}, \\
V_{f,k+1} &= \tilde{\boldsymbol{e}}_{f,k+1}^T\boldsymbol{P}_f\tilde{\boldsymbol{e}}_{f,k+1}.
\end{aligned}$$

Theorem 1. *For an assumed attenuation level μ_f of $\bar{\boldsymbol{w}}_k$, the design problem of an $\mathcal{H}_\infty$ estimator for* (1) *and* (2) *can be solved if there exist $\boldsymbol{N}_f$ and $\boldsymbol{P}_f \succ 0$, such that*

$$\begin{bmatrix} -\boldsymbol{P}_f + \boldsymbol{I} & * & * \\ \boldsymbol{0} & -\mu_f^2\boldsymbol{I} & * \\ \boldsymbol{P}_f\bar{\boldsymbol{A}}(\boldsymbol{h}) - \boldsymbol{N}_f\bar{\boldsymbol{C}} & \boldsymbol{P}_f\bar{\boldsymbol{W}}_3 - \boldsymbol{N}_f\tilde{\boldsymbol{W}}_2 & -\boldsymbol{P}_f \end{bmatrix} \prec 0. \tag{42}$$

Proof. Based on (41) it can be observed that

$$\begin{aligned}
\tilde{\boldsymbol{e}}_{f,k+1}^T\boldsymbol{P}_f\tilde{\boldsymbol{e}}_{f,k+1} - \tilde{\boldsymbol{e}}_{f,k}^T\boldsymbol{P}_f\tilde{\boldsymbol{e}}_{f,k} \\
+ \tilde{\boldsymbol{e}}_{f,k}^T\tilde{\boldsymbol{e}}_{f,k} - \mu_f^2\bar{\boldsymbol{w}}_k^T\bar{\boldsymbol{w}}_k < 0.
\end{aligned} \tag{43}$$

Thus, substituting (36) into (43) yields

$$\begin{aligned}
&\tilde{\boldsymbol{e}}_{f,k}^T\left(\bar{\boldsymbol{A}}_2(\boldsymbol{h})^T\boldsymbol{P}_f\bar{\boldsymbol{A}}_2(\boldsymbol{h}) - \boldsymbol{P}_f + \boldsymbol{I}\right)\tilde{\boldsymbol{e}}_{f,k} \\
&\quad + \tilde{\boldsymbol{e}}_{f,k}^T\left(\bar{\boldsymbol{A}}_2(\boldsymbol{h})^T\boldsymbol{P}_f\bar{\boldsymbol{W}}_2\right)\bar{\boldsymbol{w}}_k \\
&\quad + \bar{\boldsymbol{w}}_k^T\left(\bar{\boldsymbol{W}}_2^T\boldsymbol{P}_f\bar{\boldsymbol{A}}_2(\boldsymbol{h})\right)\tilde{\boldsymbol{e}}_{f,k} \\
&\quad + \bar{\boldsymbol{w}}_k^T\left(\bar{\boldsymbol{W}}_2^T\boldsymbol{P}_f\bar{\boldsymbol{W}}_2 - \mu_f^2\boldsymbol{I}\right)\bar{\boldsymbol{w}}_k < 0.
\end{aligned} \tag{44}$$

Moreover, defining

$$\bar{\boldsymbol{v}}_k = \begin{bmatrix} \tilde{\boldsymbol{e}}_{f,k}^T & \bar{\boldsymbol{w}}_k^T \end{bmatrix}^T \tag{45}$$

shows that (44) may be presented as

$$\bar{\boldsymbol{v}}_k^T = \begin{bmatrix} \bar{\boldsymbol{A}}_2(\boldsymbol{h})^T\boldsymbol{P}_f\bar{\boldsymbol{A}}_2(\boldsymbol{h}) - \boldsymbol{P}_f + \boldsymbol{I} & \\ \bar{\boldsymbol{W}}_2^T\boldsymbol{P}_f\bar{\boldsymbol{A}}_2(\boldsymbol{h}) & \\ \bar{\boldsymbol{A}}_2(\boldsymbol{h})^T\boldsymbol{P}_f\bar{\boldsymbol{W}}_2 & \\ \bar{\boldsymbol{W}}_2^T\boldsymbol{P}_f\bar{\boldsymbol{W}}_2 - \mu_f^2\boldsymbol{I} & \end{bmatrix} \bar{\boldsymbol{v}}_k \prec 0, \tag{46}$$

along with its simpler form

$$\begin{aligned}
&\begin{bmatrix} \bar{\boldsymbol{A}}_2(\boldsymbol{h})^T \\ \bar{\boldsymbol{W}}_2^T \end{bmatrix} \boldsymbol{P}_f \begin{bmatrix} \bar{\boldsymbol{A}}_2(\boldsymbol{h}) & \bar{\boldsymbol{W}}_2 \end{bmatrix} \\
&\quad + \begin{bmatrix} -\boldsymbol{P}_f + \boldsymbol{I} & \boldsymbol{0} \\ \boldsymbol{0} & -\mu_f^2\boldsymbol{I} \end{bmatrix} \prec 0.
\end{aligned} \tag{47}$$

Consequently, using the Schur complement and pre- and post-multiplying (47) by diag $(\boldsymbol{I}, \boldsymbol{I}, \boldsymbol{P}_f)$, we get

$$\begin{bmatrix} -\boldsymbol{P}_f + \boldsymbol{I} & * & * \\ \boldsymbol{0} & -\mu_f^2 \boldsymbol{I} & * \\ \boldsymbol{P}_f \bar{\boldsymbol{A}}_2(\boldsymbol{h}) & \boldsymbol{P}_f \bar{\boldsymbol{W}}_2 & -\boldsymbol{P}_f \end{bmatrix} \prec 0. \tag{48}$$

Finally, it follows easily that

$$\begin{aligned} \boldsymbol{P}_f \bar{\boldsymbol{A}}_2(\boldsymbol{h}) &= \boldsymbol{P}_f \bar{\boldsymbol{A}}(\boldsymbol{h}) - \boldsymbol{P}_f \bar{\boldsymbol{K}} \bar{\boldsymbol{C}} \\ &= \boldsymbol{P}_f \bar{\boldsymbol{A}}(\boldsymbol{h}) - \boldsymbol{N}_f \bar{\boldsymbol{C}}, \end{aligned} \tag{49}$$

$$\begin{aligned} \boldsymbol{P}_f \bar{\boldsymbol{W}}_2 &= \boldsymbol{P}_f \bar{\boldsymbol{W}}_3 - \boldsymbol{P}_f \bar{\boldsymbol{K}} \tilde{\boldsymbol{W}}_2 \\ &= \boldsymbol{P}_f \bar{\boldsymbol{W}}_3 - \boldsymbol{N}_f \tilde{\boldsymbol{W}}_2, \end{aligned} \tag{50}$$

which completes the proof. ■

Based on the above, the final procedure for the design observer consists in solving the LMIs (42) and obtaining the following gain matrices:

$$\bar{\boldsymbol{K}} = \begin{bmatrix} \boldsymbol{K}_x \\ \boldsymbol{K}_a \\ \boldsymbol{K}_s \end{bmatrix} = \boldsymbol{P}_f^{-1} \boldsymbol{N}_f. \tag{51}$$

Based on (35), assume the following form of the controller:

$$\tilde{\boldsymbol{e}}_{c,k+1} = \bar{\boldsymbol{A}}_1(\boldsymbol{h}) \tilde{\boldsymbol{e}}_{c,k} - \boldsymbol{W}_1 \bar{\boldsymbol{w}}_k. \tag{52}$$

Similarly to the observer-based system, recall the Lyapunov candidate function

$$V_{c,k} = \tilde{\boldsymbol{e}}_{c,k}^T \boldsymbol{P}_c \tilde{\boldsymbol{e}}_{c,k}, \tag{53}$$

with $\boldsymbol{P}_c \succ 0$. Additionally, we make the general assumption that $\bar{\boldsymbol{w}}_k \in l_2$ while

$$l_2 = \{\mathbf{w} \in \mathbb{R}^n | \ \|\mathbf{w}\|_{l_2} < +\infty\}, \tag{54}$$

$$\|\mathbf{w}\|_{l_2} = \left(\sum_{k=0}^{\infty} \|\boldsymbol{w}_k\|^2 \right)^{\frac{1}{2}}. \tag{55}$$

Thus, also in this case, $\bar{\boldsymbol{w}}_k$ is overbounded by the ellipsoid

$$\mathbb{E}_w = \left\{ \bar{\boldsymbol{w}}_k : \ \bar{\boldsymbol{w}}_k^T \frac{\mu_c^2}{\alpha} \boldsymbol{I} \bar{\boldsymbol{w}}_k \le 1 \right\}, \tag{56}$$

with

$$\frac{\mu_c^2}{\alpha} \boldsymbol{I} \succ 0.$$

Finally, define the following stability condition for the controller system:

$$\Delta V_{c,k} + \tilde{\boldsymbol{e}}_{c,k}^T \tilde{\boldsymbol{e}}_{c,k} - \mu_c^2 \bar{\boldsymbol{w}}_k^T \bar{\boldsymbol{w}}_k < 0, \tag{57}$$

along with

$$\begin{aligned} \Delta V_{c,k} &= V_{c,k+1} - V_{c,k}, \\ V_{c,k+1} &= \tilde{\boldsymbol{e}}_{c,k+1}^T \boldsymbol{P}_c \tilde{\boldsymbol{e}}_{c,k+1}. \end{aligned}$$

Theorem 2. *For an assumed attenuation level $\mu_c > 0$ of $\tilde{\boldsymbol{e}}_{c,k}$, the $\mathcal{H}_\infty$ controller design task* (22) *can be solved if there exist matrices $\boldsymbol{N}_c$, $\boldsymbol{U}_c$, $\boldsymbol{P}_c \succ 0$ such that*

$$\begin{bmatrix} -\boldsymbol{P}_c & * & * & * \\ 0 & -\mu_c^2 \boldsymbol{I} & * & * \\ \boldsymbol{A}\boldsymbol{U}_c - \boldsymbol{B}\boldsymbol{N}_c & -\boldsymbol{W}_1 & \boldsymbol{P}_c - \boldsymbol{U}_c - \boldsymbol{U}_c^T & * \\ \boldsymbol{U}_c & 0 & 0 & -\boldsymbol{I} \end{bmatrix} \prec 0. \tag{58}$$

Proof. The proof follows the technique used to prove Theorem 1. Accordingly, it is reduced to the inequality

$$\begin{bmatrix} \bar{\boldsymbol{A}}_1(\boldsymbol{h})^T \\ -\boldsymbol{W}_1^T \end{bmatrix} \boldsymbol{P}_c \begin{bmatrix} \bar{\boldsymbol{A}}_1(\boldsymbol{h}) & -\boldsymbol{W}_1 \end{bmatrix} + \begin{bmatrix} -\boldsymbol{P}_c + \boldsymbol{I} & \boldsymbol{0} \\ \boldsymbol{0} & -\mu_c^2 \boldsymbol{I} \end{bmatrix} \prec 0, \tag{59}$$

which can be used to derive (58) based on the method expressed in Theorem 1 by Witczak *et al.* (2016a). ■

Concluding, the design procedure of the controller system is reduced to solving the LMIs (58) and calculating

$$\boldsymbol{K}_c = \boldsymbol{N}_c \boldsymbol{U}_c^{-1}. \tag{60}$$

3. Determination of uncertainty intervals

It should be emphasized that the diagnostic system, which is an indispensable part of the fault-tolerant control system, should be robust to different sources of uncertainty and disturbances. As the observer (23)–(25) provides estimates of the state as well as sensor and actuator faults, it is necessary to determine the uncertainty intervals on the basis of state and fault bounds obtained with the basis input-output data set. Such intervals can be successfully used in diagnostic and fault tolerant control tasks (Witczak *et al.*, 2014; Pazera and Witczak, 2019). To solve such a challenging problem, we need the following result:

Corollary 1. *If* (52) *satisfies* (58)*, then there exists $0 < \gamma < 1$ such that, for all admissible $\bar{\boldsymbol{w}}_k \in \mathbb{E}_w$,*

$$V_{c,k} \le \beta_k(\gamma) \quad k = 0, 1, \ldots, \tag{61}$$

with

$$\beta_k(\gamma) = (1-\gamma)^k \tilde{\boldsymbol{e}}_{c,k} \boldsymbol{P}_c \tilde{\boldsymbol{e}}_{c,k} + \mu_p \sum_{i=0}^{k-1} (1-\gamma)^i, \tag{62}$$

where

$$\mu_p = \mu_c^2 \sum_{i=1}^{n+ns+r} q_{w,i,i}^{-1}. \tag{63}$$

The obtained upper bound makes it possible to formulate a general result allowing to determine the uncertainty intervals.

Theorem 3. (Pazera and Witczak, 2019) *Assume that*

$$V_{f,k} \leq \eta_k. \tag{64}$$

Then the uncertainty intervals for the state, sensor and actuator faults can be calculated according to the following expressions:

$$\hat{\boldsymbol{x}}_{i,f,k} - \boldsymbol{s}_{f,i,k} \leq \boldsymbol{x}_{i,f,k} \leq \hat{\boldsymbol{x}}_{i,f,k} + \boldsymbol{s}_{f,i,k}, \quad i = 1, \ldots, n, \tag{65}$$

$$\hat{\boldsymbol{f}}_{j,s,k} - \boldsymbol{s}_{f,i,k}, \leq \boldsymbol{f}_{j,s,k} \leq \hat{\boldsymbol{f}}_{j,s,k} + \boldsymbol{s}_{f,i,k}, \quad j = 1, \ldots, ns, \; i = n+1, \ldots, n+ns, \tag{66}$$

$$\hat{\boldsymbol{f}}_{l,a,k} - \boldsymbol{s}_{f,i,k}, \leq \boldsymbol{f}_{l,a,k} \leq \hat{\boldsymbol{f}}_{l,a,k} + \boldsymbol{s}_{f,i,k}, \quad l = 1, \ldots, na, \; i = n+ns+1, \ldots, n+ns+r, \tag{67}$$

where

$$\boldsymbol{s}_{f,i,k} = \left(\eta_k \boldsymbol{c}_{f,i}^T \boldsymbol{P}_f^{-1} \boldsymbol{c}_{f,i}\right)^{\frac{1}{2}}. \tag{68}$$

The coefficient $\boldsymbol{c}_{f,i}$ represents the i-th column of the identity matrix of size $n + ns + na$.

Theorem 4. *Assume that*

$$V_{c,k} \leq \eta_k. \tag{69}$$

The uncertainty intervals of the tracking error satisfy

$$-\boldsymbol{s}_{c,i,k} \leq \boldsymbol{e}_{i,k} \leq \boldsymbol{s}_{c,i,k}, \quad i = 1, \ldots, n.$$

Proof. From (57) we have

$$V_{c,k+1} - V_{c,k} < \mu_c^2 \bar{\boldsymbol{w}}_k^T \bar{\boldsymbol{w}}_k - \tilde{\boldsymbol{e}}_{c,k}^T \tilde{\boldsymbol{e}}_{c,k}. \tag{70}$$

Since $\bar{\boldsymbol{w}}_k \in \mathbb{E}_w$, i.e., $\bar{\boldsymbol{w}}_k^T \boldsymbol{Q}_w \bar{\boldsymbol{w}}_k \leq 1$, we deduce that

$$V_{c,k+1} < \mu_{c,p} + V_{c,k} - \tilde{\boldsymbol{e}}_{c,k}^T \tilde{\boldsymbol{e}}_{c,k}, \tag{71}$$

or

$$V_{c,k+1} < \mu_{c,p} + \tilde{\boldsymbol{e}}_{c,k}^T \left(\boldsymbol{P}_c - \boldsymbol{I}\right) \tilde{\boldsymbol{e}}_{c,k}. \tag{72}$$

If condition (58) is satisfied, then $\boldsymbol{P}_c - \boldsymbol{I} > 0$, which yields

$$\tilde{\boldsymbol{e}}_{c,k}^T \boldsymbol{P}_c \tilde{\boldsymbol{e}}_{c,k} > \tilde{\boldsymbol{e}}_{c,k}^T \tilde{\boldsymbol{e}}_{c,k}. \tag{73}$$

Hence there exists $0 < \zeta < 1$ such that

$$\gamma \tilde{\boldsymbol{e}}_{c,k}^T \boldsymbol{P}_c \tilde{\boldsymbol{e}}_{c,k} = \tilde{\boldsymbol{e}}_{c,k}^T \tilde{\boldsymbol{e}}_{c,k}. \tag{74}$$

Equations (74) and (72) lead to

$$V_{c,k+1} \leq \mu_{c,p} + (1 - \gamma) V_{c,k}. \tag{75}$$

By applying induction, (75) is a counterpart to (62), which completes the proof. ∎

It should be emphasised that the parameter γ in (74) can be achieved by applying the Rayleigh quotient, i.e.,

$$\gamma = \frac{\tilde{\boldsymbol{e}}_{c,k}^T \tilde{\boldsymbol{e}}_{c,k}}{\tilde{\boldsymbol{e}}_{c,k}^T \boldsymbol{P}_c \tilde{\boldsymbol{e}}_{c,k}} \leq \lambda_{\min}(\boldsymbol{P}_c)^{-1}, \tag{76}$$

where $\lambda_{\min}(\boldsymbol{P}_c)$ stands for the minimum eigenvalue of $\boldsymbol{P}_c$.

Summarizing, the developed boundaries are calculated analytically based on the fault estimates with addition of the factor calculated directly from the observer/controller gain matrix according to (65)–(67). In the case of actuator faults, if it is assumed that 0 means that there is no fault, and 1 stands for a failure, there is a possibility to achieve a maximum boundary of the actuator fault. In the case of a sensor fault, it is impossible to determine the exact value of the maximum fault since its faulty condition may yield a wide spectrum of values.

4. Illustrative example

The effectiveness of the proposed FTTC strategy was tested with a laboratory twin-rotor aerodynamical system (TRAS), presented in Fig. 2. This system was used to practically validate identification, fault diagnosis as well as the control strategy for nonlinear systems. The TRAS can be represented by a 6th order highly nonlinear model. Its full model description is omitted due to the lack of space; nevertheless, all details can be found in the work of Witczak *et al.* (2016b).

The system state $\boldsymbol{x}$ vector is given as

$$\boldsymbol{x} = \left[\theta_h, \theta_v, \omega_h, \Omega_h, \Omega_v, \omega_v\right]^T, \tag{77}$$

where

- θ_h is the yaw angle of the beam,
- θ_v is the pitch angle of the beam,
- ω_h is the rotational velocity of the tail rotor,

Fig. 2. Laboratory twin-rotor aerodynamical system.

- Ω_h is the angular velocity of the tail rotor,
- Ω_v is the angular velocity of the main rotor,
- ω_v is the rotational velocity of the main rotor.

Moreover, the input vector is defined as

$$\boldsymbol{u} = [u_v, u_h]^T, \tag{78}$$

where $\boldsymbol{u}_v$ and $\boldsymbol{u}_h$ signify the control inputs resulting from the main and tail DC motors, respectively. The system is controlled via a personal computer which communicates with it by a dedicated I/O board controlled by real-time software operated by a Matlab/Simulink. For more details about the used TRAS system, the reader is referred to INTECO (2007).

Assume the following fault scenario:

$$\boldsymbol{f}_{a,1,k} = \begin{cases} 0, & 1 \le k \le 1000, \\ a \cdot e^{bj} \cdot \boldsymbol{u}_{f,k}, & 1001 \le k \le 16000, \\ j = 1, 2, \ldots, 15000, & \\ -1, & 16001 \le k \le 19000, \end{cases} \tag{79}$$

where $a = 40.5 \cdot 10^{-4}, b = 7.14 \cdot 10^{-4}$,

$$\boldsymbol{f}_{a,2,k} = 0, \tag{80}$$

$$\boldsymbol{f}_{s,1,k} = \begin{cases} \boldsymbol{y}_{f,k} + 2.8, & 7000 \le k \le 11000, \\ 0, & \text{otherwise}, \end{cases} \tag{81}$$

$$\boldsymbol{f}_{s,2,k} = \begin{cases} \boldsymbol{y}_{f,k} - 1.5, & 9000 \le k \le 14000, \\ 0, & \text{otherwise}, \end{cases} \tag{82}$$

along with the distribution matrices of external disturbances for the process and measurement uncertainties

$$\boldsymbol{W}_1 = 1 \cdot 10^{-3}\boldsymbol{I}, \quad \boldsymbol{W}_2 = 5 \cdot 10^{-2}\boldsymbol{I}. \tag{83}$$

The distribution matrix of sensor faults is

$$\boldsymbol{C}_f = \begin{bmatrix} 0 & 0 & 0 & 1 & 0 & 0 \\ 0 & 0 & 0 & 0 & 1 & 0 \end{bmatrix}^T, \tag{84}$$

which means that sensor faults in the Ω_h and Ω_v states. From the fault scenario, it can be observed that the actuator fault is exponential, which means that the fault is increasing due to the failure ($\boldsymbol{f}_{a,1,k} = -1$). Nevertheless, the sensor faults are steady and either negative or positive. Accordingly, it can be observed that the actuator and sensor faults influenced the system simultaneously.

Figures 3–5 confirm the correctness of the actuator and sensor fault estimation. Thus, it can be easily observed that the faults are estimated with a very good accuracy. The estimates properly follow the real faults even in the presence of external disturbances. Moreover, the states are presented in Figs. 6–11. The reference states are correctly estimated and in consequence, the

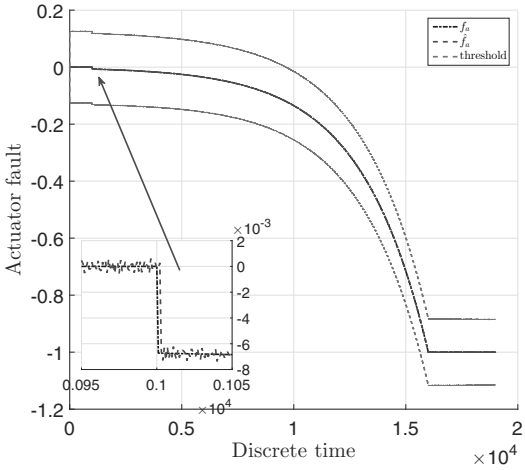

Fig. 3. Actuator fault $\boldsymbol{f}_{a,1,k}$.

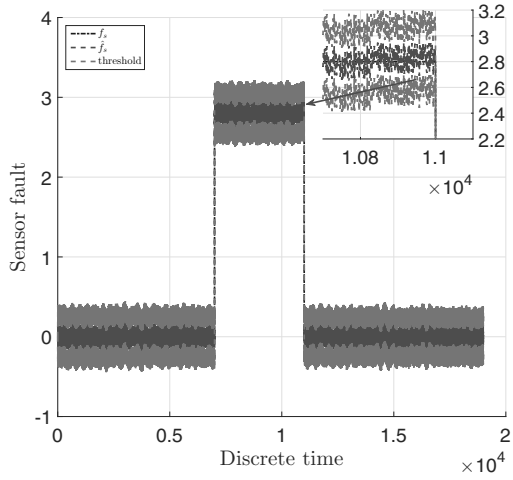

Fig. 4. Sensor fault $\boldsymbol{f}_{s,1,k}$.

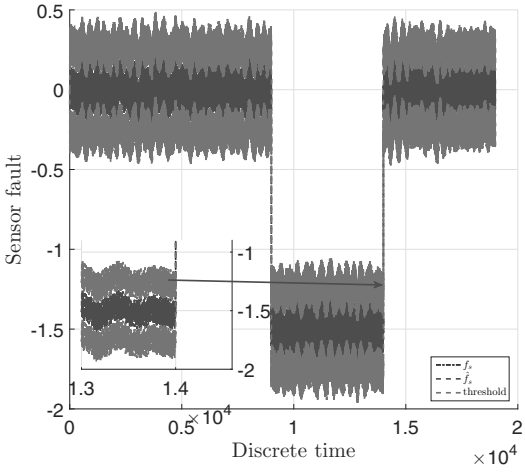

Fig. 5. Sensor fault $\boldsymbol{f}_{s,2,k}$.

Table 1. Mean value and mean squared error of the estimation and tracking errors.

State	Estimation error		Tracking error	
	Mean value	Mean squared error	Mean value	Mean squared error
θ_h [rad]	$2.5498 \cdot 10^{-5}$	$6.2235 \cdot 10^{-6}$	0.4680	4.6650
θ_v [rad]	$2.3879 \cdot 10^{-4}$	$2.8120 \cdot 10^{-5}$	0.1550	0.4254
ω_h [RPM]	-0.0162	0.0199	10.2880	$1.6844 \cdot 10^{3}$
Ω_h [rad/s]	$4.4098 \cdot 10^{-4}$	$4.5475 \cdot 10^{-4}$	$3.7337 \cdot 10^{-5}$	$4.5859 \cdot 10^{-4}$
Ω_v [rad/s]	0.0014	0.0014	-0.0014	0.0014
ω_v [RPM]	$1.2228 \cdot 10^{-4}$	0.0210	-0.0045	0.0048
$\boldsymbol{f}_{a,1,k}$	$-1.0588 \cdot 10^{-4}$	$1.3256 \cdot 10^{-7}$	n/a	n/a
$\boldsymbol{f}_{a,2,k}$	$3.4824 \cdot 10^{-7}$	$2.2478 \cdot 10^{-6}$	n/a	n/a
$\boldsymbol{f}_{s,1,k}$	$2.3851 \cdot 10^{-4}$	0.0066	n/a	n/a
$\boldsymbol{f}_{s,2,k}$	-0.0018	0.0075	n/a	n/a

state with the fault-tolerant controller correctly imitates the reference state also in the case when actuator and sensor faults or external disturbances are present.

It is worth emphasizing that the nominal controller does not track the reference state due to the occurrence of the actuator fault. An important thing to note is that the fault-tolerant controller stops following the reference state when the actuator fault is equal to -1, which means that a failure occurred and the actuator stops working. Accordingly, it is not possible to control the system while the actuator is totally broken. Moreover, Figs. 12 and 13 provide the control comparison between the nominal $\boldsymbol{u}_k$ and fault-tolerant $\boldsymbol{u}_{f,k}$ controller. It can be easily observed that the control signal of the fault-tolerant controller is increasing due to the fact that so is the actuator fault. In the other hand, the control signal of the nominal controller is steady. Finally, Figs. 14 and 15 indicate the tracking error for all the states given with solid lines, while their uncertainty intervals are given with dashed lines. Accordingly, the tracking error for all states are near zero until the actuator is totally broken. Moreover, the tracking errors are overbounded by the bounds defined in Section 3, which ensures that the tracking errors are inside these bounds. Additionally, the mean value and the mean squared error of the estimation and tracking errors are presented in Table 1, which proves the correctness and good performance of the proposed approach.

5. Conclusions

The paper has dealt with the design problem of a control strategy for nonlinear systems which are affected by actuator and sensor faults along with simultaneously measurement and process uncertainties. An important feature of the proposed approach is that it can be used along with the already existing control strategy, which means that the existing controller may be considered as a nominal one. Thus, to achieve the proposed control strategy, there was a need to design a robust observer, which is capable to estimate the state as well as actuator and sensor faults. Based on the achieved estimates, the proposed fault-tolerant tracking controller allows us to minimize the tracking error between the reference state and the state of the possibly faulty system. Additionally, the uncertainty intervals were defined for the estimation quality assessment, while these intervals overbound the state, actuator and sensor faults as well as the tracking error. Consequently, the uncertainty interval of a fault may be considered instead of using a point estimate. Thus, more reliable decisions can be performed.

Finally, the proposed fault-tolerant tracking control strategy was verified by using the 6th order highly nonlinear model of a twin rotor aerodynamical laboratory system. Accordingly, the proposed fault scenario included actuator and sensor faults simultaneously with external disturbances. Concluding, the obtained results clearly confirm the performance and correctness of the proposed fault-tolerant control strategy. Future research directions are oriented towards extending the proposed approach with a suitable mechanism capable of determining the remaining useful life of the actuators. For that purpose, a degradation model has to be determined while its parameters have to be constantly updated with the proposed fault estimation strategy. Another research direction is oriented towards applying the proposed strategy for fault estimation, control and remaining useful life estimation for a fleet of vehicles. Such an approach allows a balanced use of such a fleet, which will make it capable of keeping an average remaining useful lifetime at a possible high level.

Acknowledgment

The work was supported by the National Science Centre, Poland, under the grant UMO-2017/27/B/ST7/00620.

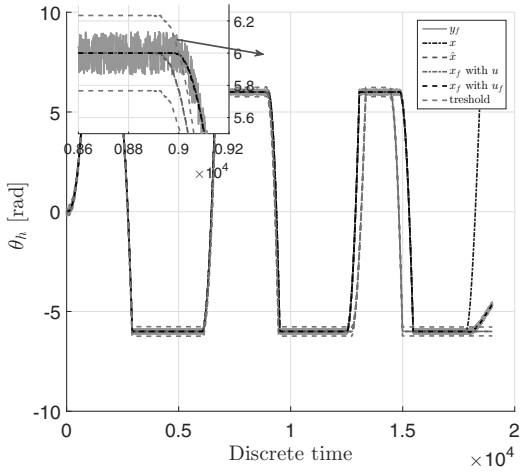

Fig. 6. Yaw angle of the beam θ_h.

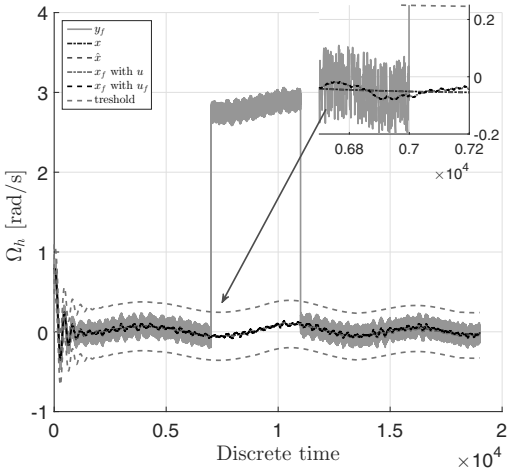

Fig. 9. Tail rotor angular velocity Ω_h.

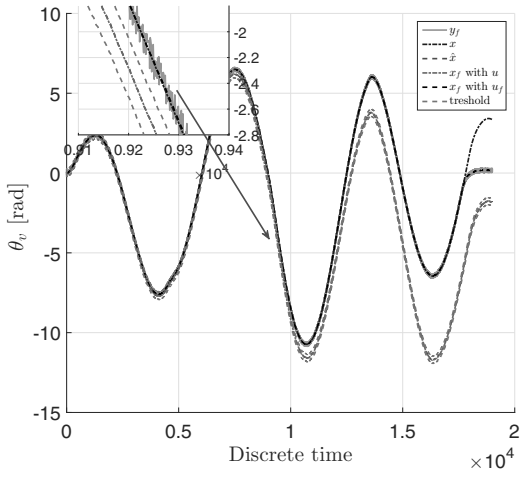

Fig. 7. Beam pitch angle θ_v.

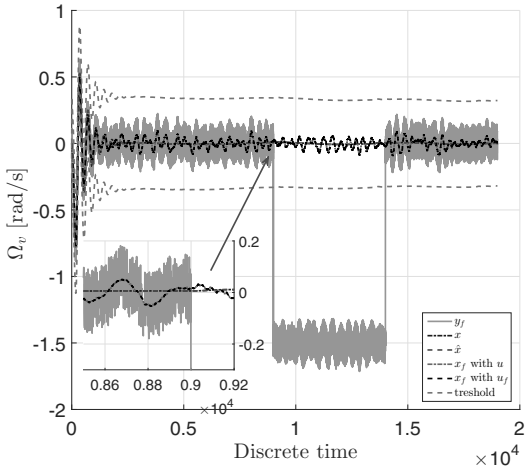

Fig. 10. Main rotor angular velocity Ω_v.

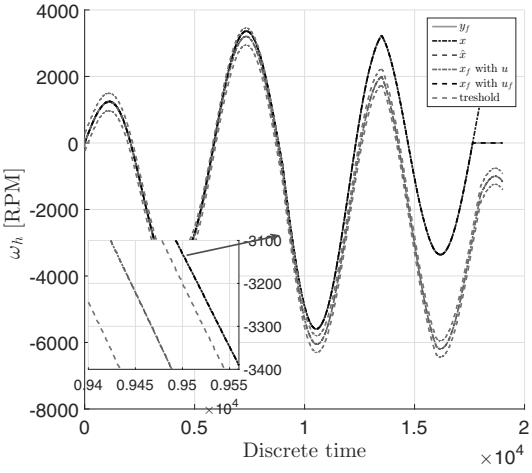

Fig. 8. Tail rotor rotational velocity ω_h.

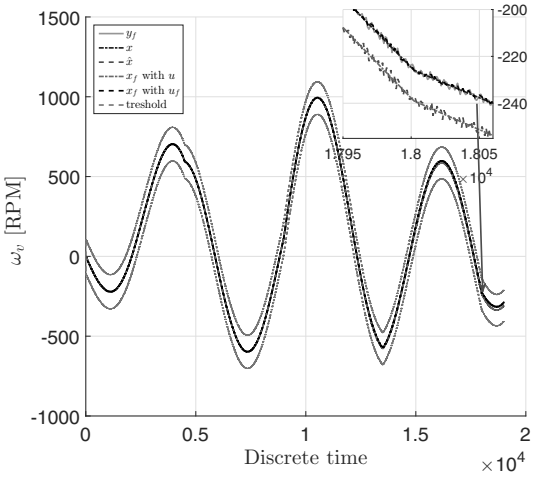

Fig. 11. Main rotor rotational velocity ω_v.

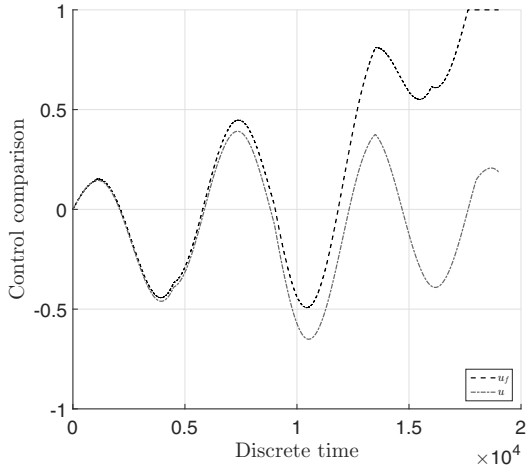

Fig. 12. Control comparison between nominal $\boldsymbol{u}_{1,k}$ and fault-tolerant controller $\boldsymbol{u}_{f,1,k}$.

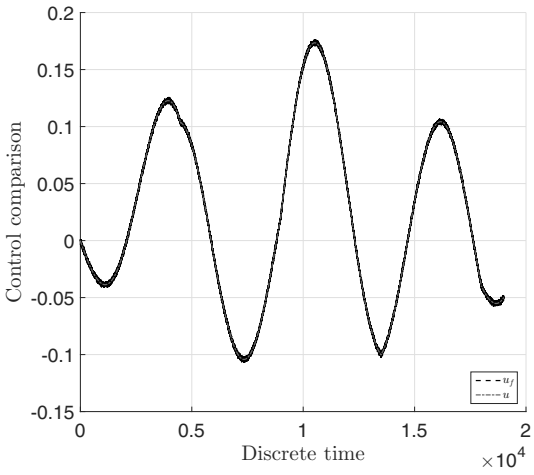

Fig. 13. Control comparison between $\boldsymbol{u}_{2,k}$ and fault-tolerant controller $\boldsymbol{u}_{f,2,k}$.

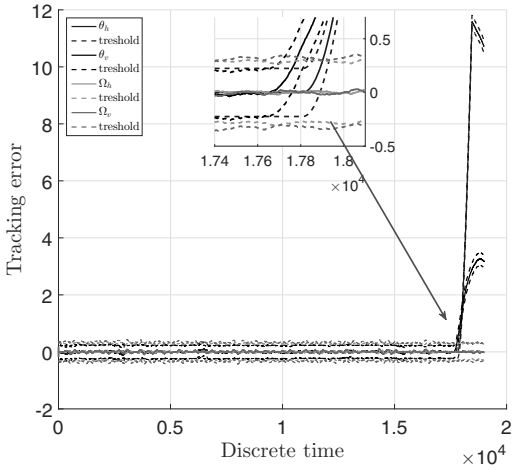

Fig. 14. Tracking errors with the uncentainty intervals for the angular velocities of the tail Ω_h and main rotor Ω_v as well as yaw θ_h and pitch θ_v angles of the beam.

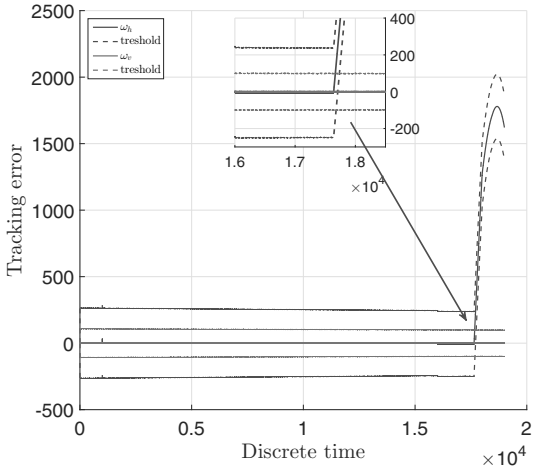

Fig. 15. Tracking errors with the uncentainty intervals for the rotational velocities of the tail, ω_h, and main rotor ω_v.

References

Abbaspour, A., Yen, K.K., Forouzannezhad, P. and Sargolzaei, A. (2018). A neural adaptive approach for active fault-tolerant control design in UAV, *IEEE Transactions on Systems, Man, and Cybernetics: Systems* **50**(9): 3401–3411.

Altan, A. and Hacıoğlu, R. (2020). Model predictive control of three-axis gimbal system mounted on UAV for real-time target tracking under external disturbances, *Mechanical Systems and Signal Processing* **138**(2020): 106548.

Azzoug, Y., Sahraoui, M., Pusca, R., Ameid, T., Romary, R. and Cardoso, A.J.M. (2021). Current sensors fault detection and tolerant control strategy for three-phase induction motor drives, *Electrical Engineering* **103**(2): 881–898.

Camci, F., Medjaher, K., Atamuradov, V. and Berdinyazov, A. (2019). Integrated maintenance and mission planning using remaining useful life information, *Engineering Optimization* **51**(10): 1794–1809.

Chen, F., Gong, J. and Li, Y. (2019). Adaptive diagnosis and compensation for hypersonic flight vehicle with multisensor faults, *International Journal of Robust and Nonlinear Control* **29**(17): 6145–6163.

Chung, W. and Son, H. (2020). Fault-tolerant control of multirotor UAVs by control variable elimination, *IEEE/ASME Transactions on Mechatronics* **25**(5): 2513–2522.

Habibi, H., Howard, I. and Simani, S. (2019). Reliability improvement of wind turbine power generation using model-based fault detection and fault tolerant control: A review, *Renewable Energy* **135**(2019): 877–896.

Hamadi, H., Lussier, B., Fantoni, I., Francis, C. and Shraim, H. (2020). Comparative study of self tuning, adaptive

and multiplexing FTC strategies for successive failures in an octorotor UAV, *Robotics and Autonomous Systems* **133**(2020): 103602.

Hamdi, H., Rodrigues, M., Rabaoui, B. and Benhadj Braiek, N. (2021). A fault estimation and fault-tolerant control based sliding mode observer for LPV descriptor systems with time delay, *International Journal of Applied Mathematics and Computer Science* **31**(2): 247–258, DOI: 10.34768/amcs-2021-0017.

Hu, K., Li, W. and Cheng, Z. (2021). Fuzzy adaptive fault diagnosis and compensation for variable structure hypersonic vehicle with multiple faults, *PLOS ONE* **16**(8): e0256200.

INTECO (2007). *Two Rotor Aerodynamical System: User's Manual*, INTECO, Kraków.

Kukurowski, N., Pazera, M. and Witczak, M. (2021). Fault-tolerant tracking control and remaining useful life estimation for Takagi–Sugeno fuzzy system, *2021 IEEE International Conference on Fuzzy Systems (FUZZ-IEEE), Luxembourg*, pp. 687–693.

Li, L., Luo, H., Ding, S.X., Yang, Y. and Peng, K. (2019). Performance-based fault detection and fault-tolerant control for automatic control systems, *Automatica* **99**(2019): 308–316.

Liu, F., Tang, H., Luo, J., Bai, L. and Pu, H. (2021). Fault-tolerant control of active compensation toward actuator faults: An autonomous underwater vehicle example, *Applied Ocean Research* **110**(2021): 102597.

Manohar, M. and Das, S. (2020). Notice of removal: Current sensor fault-tolerant control of induction motor driven electric vehicle using flux-linkage observer, *2020 IEEE Transportation Electrification Conference & Expo (ITEC), Chicago, USA*, pp. 884–889.

Mrugalski, M. (2014). *Advanced Neural Network-based Computational Schemes for Robust Fault Diagnosis*, Springer, Berlin.

Nguyen, D.-T., Saussié, D. and Saydy, L. (2017). Robust self-scheduled fault-tolerant control of a quadrotor UAV, *IFAC-PapersOnLine* **50**(1): 5761–5767.

Patel, H.R. and Shah, V.A. (2019). A passive fault-tolerant control strategy for a non-linear system: An application to the two tank conical non-interacting level control system, *Maskay* **9**(1): 1–8.

Pazera, M. and Witczak, M. (2019). Towards robust simultaneous actuator and sensor fault estimation for a class of nonlinear systems: Design and comparison, *IEEE Access* **7**: 97143–97158.

Petritoli, E., Leccese, F. and Ciani, L. (2018). Reliability and maintenance analysis of unmanned aerial vehicles, *Sensors* **18**(9): 3171.

Prochazka, K.F. and Stomberg, G. (2020). Integral sliding mode based model reference FTC of an over-actuated hybrid UAV using online control allocation, *2020 American Control Conference (ACC), Denver, USA*, pp. 3858–3864.

Rodrigues, L.R., Gomes, J.P. and Alcântara, J.F. (2018). Embedding remaining useful life predictions into a modified receding horizon task assignment algorithm to solve task allocation problems, *Journal of Intelligent & Robotic Systems* **90**(1): 133–145.

Sadhu, V., Zonouz, S. and Pompili, D. (2020). On-board deep-learning-based unmanned aerial vehicle fault cause detection and identification, *2020 IEEE International Conference on Robotics and Automation (ICRA), Paris, France*, pp. 5255–5261.

Saied, M., Lussier, B., Fantoni, I., Shraim, H. and Francis, C. (2020). Active versus passive fault-tolerant control of a redundant multirotor UAV, *Aeronautical Journal* **124**(1273): 385–408.

Sun, K. and Liu, X. (2021). Path planning for an autonomous underwater vehicle in a cluttered underwater environment based on the heat method, *International Journal of Applied Mathematics and Computer Science* **31**(2): 289–301, DOI: 10.34768/amcs-2021-0020.

Taimoor, M., Lu, X., Maqsood, H. and Sheng, C. (2021). Adaptive rapid neural observer-based sensors fault diagnosis and reconstruction of quadrotor unmanned aerial vehicle, *Aircraft Engineering and Aerospace Technology* **93**(5): 847–861.

Tang, H., Chen, Y. and Zhou, A. (2021). Actuator fault-tolerant control for four-wheel-drive-by-wire electric vehicle, *IEEE Transactions on Transportation Electrification* **8**(2): 2361–2373.

Veremey, E.I. (2021). An approximate solution of the affine-quadratic control problem based on the concept of optimal damping, *International Journal of Applied Mathematics and Computer Science* **31**(1): 5–15, DOI: 10.34768/amcs-2021-0001.

Vural, S.Y., Dasdemir, J. and Hajiyev, C. (2018). Passive fault tolerant lateral controller design for an UAV, *IFAC-PapersOnLine* **51**(30): 446–451.

Wang, X. (2020). Active fault tolerant control for unmanned underwater vehicle with sensor faults, *IEEE Transactions on Instrumentation and Measurement* **69**(12): 9485–9495.

Witczak, M. (2014). *Fault Diagnosis and Fault-Tolerant Control Strategies for Non-Linear Systems*, Springer, Heidelberg.

Witczak, M., Buciakowski, M. and Aubrun, C. (2016a). Predictive actuator fault-tolerant control under ellipsoidal bounding, *International Journal of Adaptive Control and Signal Processing* **30**(2): 375–392.

Witczak, M., Buciakowski, M. and Mrugalski, M. (2014). An H_infinity approach to fault estimation of non-linear systems: application to one-link manipulator, *Methods and Models in Automation and Robotics, MMAR, Międzyzdroje, Poland*, pp. 456–461.

Witczak, M., Buciakowski, M., Puig, V., Rotondo, D. and Nejjari, F. (2016b). An LMI approach to robust fault estimation for a class of nonlinear systems, *International Journal of Robust and Nonlinear Control* **26**(7): 1530–1548.

Witczak, M., Mrugalski, M., Pazera, M. and Kukurowski, N. (2020). Fault diagnosis of an automated guided vehicle with torque and motion forces estimation: A case study, *ISA Transactions* **104**(2020): 370–381.

Yu, Z., Zhang, Y., Jiang, B., Su, C.-Y., Fu, J., Jin, Y. and Chai, T. (2021). Nussbaum-based finite-time fractional-order backstepping fault-tolerant flight control of fixed-wing UAV against input saturation with hardware-in-the-loop validation, *Mechanical Systems and Signal Processing* **153**(2021): 107406.

Zemouche, A. and Boutayeb, M. (2013). On LMI conditions to design observers for Lipschitz nonlinear systems, *Automatica* **49**(2): 585–591.

Zhang, X., Zhao, Z., Wang, Z. and Wang, X. (2021). Fault detection and identification method for quadcopter based on airframe vibration signals, *Sensors* **21**(2): 581.

Norbert Kukurowski was born in 1994 in Poland. He received his MSc degree in control engineering and robotics from the University of Zielona Góra (Poland) in 2018. He is currently a PhD student at the Institute of Control and Computation Engineering there. His present research interests include fault diagnosis, fault-tolerant control as well as diagnostic of process and systems.

Marcin Mrugalski was born in Poland in 1975. He received his MSc and PhD degrees in electrical engineering from the University of Zielona Góra, Poland, in 1999 and 2004, respectively. He obtained his DSc degree in computer science from the Częstochowa University of Technology, Poland, in 2014. He has been an associate professor of automatic control and robotics at the Institute of Control and Computation Engineering, University of Zielona Góra, since 2014. He has published one monograph and more than 70 papers in international journals, book chapters and conference proceedings. His current research interests include neural networks, computational intelligence, fault diagnosis and fault tolerant control.

Marcin Pazera was born in Poland in 1990. He received his MSc degree in control engineering and robotics from the University of Zielona Góra (Poland) in 2015. He is currently a PhD student at the Institute of Control and Computation Engineering there. His present research interests include fault detection and isolation (FDI) and fault-tolerant control (FTC).

Marcin Witczak was born in Poland in 1973. He received his MSc degree in electrical engineering from the University of Zielona Góra (Poland), his PhD degree in automatic control and robotics from the Wrocław University of Technology (Poland), and his DSc degree in electrical engineering from the University of Zielona Góra, in 1998, 2002 and 2007, respectively. In 2015 he obtained a full professorial title. Since then, Marcin Witczak has been a professor of automatic control and robotics at the Institute of Control and Computation Engineering, University of Zielona Góra. His current research interests include computational intelligence, fault detection and isolation (FDI), fault-tolerant control (FTC), as well as experimental design and control theory. Marcin Witczak has published more than 200 papers in international journals and conference proceedings. He has authored four monographs and 30 book chapters. Since 2015, he has been a member of the Committee on Automatic Control and Robotics of the Polish Academy of Sciences. Since 2018, he has also been an associate editor of *ISA Transactions*.

Received: 28 December 2021
Revised: 15 February 2022
Accepted: 9 May 2022